The Role of Surface Passivation in Controlling the Chemistry and Adhesion at the Interface of Bitumen and Siliceous Surfaces

Albert M. Hung, [a] Farideh Pahlavan[a], Sheyda Shakiba,[b] Shery L. Y. Chang[c], Stacey M. Louie,[b] Elham H. Fini[c,*]
a. North Carolina A&T State University, 1601 E. Market St., Greensboro, NC 27401, USA
b. University of Houston, 4726 Calhoun Rd., Houston, TX 77204-4003, USA
c. Arizona State University, Tempe, AZ 85287-3005, Phone: 480-965-4273, USA

* Corresponding author: E. H. Fini (efini@asu.edu)

ABSTRACT

Good adhesion between bitumen and aggregate is critical for the durability of asphalt pavement, but adhesion is fundamentally governed by interface-specific molecular migration, adsorption, and bonding phenomena of which there is limited understanding. This paper examines the efficacy of an amide-rich Bio-binder or other compounds derived from bio-residue as dopants in bitumen to control passivation of the interface of bitumen and siliceous stone aggregates. Acid compounds in bitumen are implicated in the increased risk of moisture damage at the bitumen-aggregate interface; the accumulation and crystallization of alkane acids at the interface of bitumen and siliceous aggregates are known to increase the propensity for moisture damage. The bio-derived dopant was effective at preventing alkane acid crystallization at the bitumen-silica interface, possibly through passivation of surface binding sites. Being able to out-compete acid compounds for binding to these sites may be a critical requirement for effective anti-stripping agents. The adsorption of layers of bio-derived compounds on siliceous surfaces was observed by TEM and *in-situ* ATR-FTIR; the primary surface-active compounds appeared to share chemical characteristics with asphaltenes found in bitumen. Moreover, DFT analysis showed specific bio-derived molecules have high binding energy to silica, which may explain their selective adsorption. The study results reveal how effective surface passivation can prevent crystallization of acids at the interface of bitumen and siliceous stones to enhance resistance to moisture damage. The outcome of this study can enhance sustainability in construction by providing an in-depth understanding of surface passivation as a means of avoiding the crystallization and subsequent hydrolyzation of acids at the interface of bitumen and stone aggregate as a means of preventing moisture damage in pavements.

Keywords: bitumen, aggregate, interface, asphaltene, microstructure, AFM, TEM, FTIR, adsorption, nanoparticle

INTRODUCTION

Petroleum-based binder (bitumen) is used to hold together mineral aggregate in applications such as the construction of pavement and the production of roof shingles. For any composite material, the properties of the interface between the mixed components is critical, and poor adhesion between bitumen and the mineral aggregate is a persistent and pervasive mode of failure in these materials. As added complications, adhesion needs to be maintained in both dry

and wet environments, and the bitumen and the aggregate can each vary dramatically in precise chemical composition.

Damage in asphalt concrete often occurs when the bonds within the bitumen binder break (cohesive failure) or when the bonds between bitumen and aggregate break (adhesive failure). Adhesion depends on the composition and microstructure of the bitumen-mineral interface, and an in-depth understanding of the interactions between bitumen components and mineral surfaces is invaluable for developing strategies to improve adhesion and the resistance to moisture damage.[1-4] Good adhesion requires not only strong bonding between the mineral surface and the adsorbed compounds but also strong bonding between the adsorbed compounds and the bulk bitumen. If the adsorbed species are too chemically distinct from the bulk mixture, then phase separation at the aggregate interface could occur, leading to de-bonding of the adsorbed layer from the bitumen.

Petroleum asphaltenes are defined as the heptane-insoluble fraction of crude oil, typically consisting of the largest and most polarizable molecules in crude oil. Asphaltene adsorption to mineral and metal surfaces is very strong and is a primary cause of issues with flow assurance in petroleum production.[5-6] Bitumen asphaltenes are also defined as the heptane-insoluble fraction and are chemically similar to petroleum asphaltenes. While asphaltene precipitation is detrimental to crude oil extraction and distribution, asphaltene adsorption may play a critical role in bitumen adhesion. Asphaltenes are typically comprised of polyaromatic hydrocarbon (PAH) cores of multiple fused aromatic rings decorated with alkane chains and other chemical groups along their periphery. There may be a single PAH core of 6-7 fused rings on average ("island-type") or a few smaller PAH cores linked together ("archipelago-type").[7-9] Polar asphaltenes that contain nitrogen and oxygen groups are particularly surface active. It is believed that these polar groups interact through strong ionic, dipole-dipole, or hydrogen bonding interactions to active sites on the mineral surface such as surface hydroxyl groups or charge centers.

Not all polar chemical groups are beneficial for adhesion. Carboxylic acid compounds may bind strongly to mineral surfaces under dry conditions but can desorb readily under water and increase the moisture susceptibility of asphalt concrete.[10-11] Additives such as hydrated lime[10, 12] or amine-based anti-stripping agents[13-16] that have shown efficacy in improving moisture damage resistance in asphalt concrete are believed to be able to bind and neutralize carboxylic acids. The surface activity of acid compounds was also observed in mixtures of bitumen with saturated fatty acids, wherein the excess acid was observed to accumulate and crystallize at the bitumen-glass interface.[17] However, carboxylic acids are not entirely detrimental to material properties. For example, the biological adhesives used by marine mussels to attach themselves to underwater rocks contain a significant concentration of both carboxylic acid and amine groups.[18-20] These groups are believed to contribute to the cohesive strength of the material by forming strong ionic bridges with each other. Thus, an effective anti-stripping treatment needs to be able to displace carboxylic acids from the aggregate surface but does not need to eliminate them entirely.

Alternative adhesion promotors derived from renewable resources or waste streams are of interest for reducing the cost and environmental impact of pavement construction. [21] These agents are often a complex mixture of different compounds, any of which may be beneficial or detrimental to adhesion.[22-24] Identification of the active compounds and their mechanism of action would be invaluable for developing more effective agents to promote adhesion.[23]In this study, the chemical adsorption of a bio-based bitumen additive to silica surfaces was characterized by microscopy, spectroscopy, and computational modeling. Atomic force

microscopy (AFM) was used to study adsorption of Bio-binder and a model carboxylic acid compound to silica. Separately, Bio-binder was adsorbed to silica nanoparticles in order to identify the chemical characteristics of the most surface-active compounds through infrared and UV-vis absorption spectroscopy, transmission electron microscopy (TEM), and electron energy loss spectroscopy (EELS). Density functional theory (DFT) computational modeling was also used to calculate the binding energies of selected chemical compounds in order to provide additional context for the experimental data. These methods prove useful for characterizing the chemical and physical aspects of molecular adsorption from complex mixtures. In turn, this information is important for developing more effective adhesion promotors and anti-stripping additives.

MATERIALS and METHODS

Materials

Fumed silica nanoparticles (abbreviated here as "NPs") with nominal surface area 175-225 m^2/g were obtained from Sigma-Aldrich. The bitumen was produced by the Philips 66 Wood River refinery in Roxana, IL, which receives primarily Canadian and U.S. crude oils.

Hexadecanoic acid (HDA, ≥99%), hexadecylamine (technical grade, 90%) tetrahydrofuran (THF, anhydrous, ≥99.9%, inhibitor-free, ACS grade, caution: peroxide former), hexamethyldisilazane (HMDS, ≥99%), and (3-aminopropyl)triethoxysilane (APTES, ≥98%) were obtained from Sigma-Aldrich. Hexadecanamide (≥95%) was obtained from Fisher Scientific. Acetone, ethanol, isopropanol, toluene, and ammonium hydroxide (all ACS grade) were obtained from Fisher Scientific. "Bio-binder" was derived from a bio-oil produced by hydrothermal liquefaction of swine manure as described elsewhere.[23] A small sample of bitumen asphaltenes was extracted by collecting the fraction insoluble in *n*-heptane. A similar heptane-insoluble fraction was also isolated from Bio-binder. For simplicity, this fraction is also referred to as Bio-binder "asphaltenes" despite being chemically distinct from the asphaltenes found in bitumen or petroleum.

Capillary tube sample preparation

To obtain a hydrophilic surface, long-stem glass Pasteur pipets (soda-lime glass, Fisher Scientific) were first cleaned by sequential ultrasonication for 10 min each in acetone, isopropanol, 30% ammonium hydroxide, and deionized (DI) water. The pipets were rinsed with more DI water and dried with a N_2 gas gun followed by at least 30 min of baking at 120 °C in a convection oven.

Bitumen mixtures were doped with 1 wt% of HDA as a model for acid-rich, moisture-susceptible binder. In one sample, 1 wt% Bio-binder was added to acid-doped bitumen to study the effect of a liquid dopant on HDA migration. Mixing was performed by melt-blending by hand at 120 ºC for 5 min. Immediately after mixing, the molten bitumen was sucked up the capillary stem of a pipet. A heat gun was used to keep the pipet warm while the bitumen was being drawn up, and excess bitumen on the outside of the tube was cleaned off with laboratory tissues and acetone. The bitumen-filled glass capillary tube was broken off the pipet and annealed at 120 °C for 30 min in a convection oven.

To investigate the effect of external control mechanisms, the inner surface of a glass pipet was covalently functionalized with either HMDS or APTES. Chemical surface functionalization was carried out immediately after ammonium hydroxide cleaning and rinsing but before oven baking. For APTES coating, an ethanol solution containing 2 vol% APTES and 5 vol% DI water was mixed together and allowed to sit for 5 minutes in order for the APTES to first hydrolyze.

The silane solution was then drawn up into the pipet and left to silanize the glass surface for 10 minutes. After silanization, the pipet was rinsed with isopropanol and DI water, briefly dried with a N_2 gun, and baked at 120 °C in a convection oven for 15 minutes to cure the coating. For HMDS coating, a similar procedure was followed using a solution of 2 vol% HMDS in toluene and without the 5-minute hydrolyzation step.

SiO_2 Nanoparticles (SiO_2 NPs) treated with Bio-binder

To further characterize the Bio-binder compounds that adsorb to silica surfaces, larger quantities of SiO_2 NPs were treated with Bio-binder and examined by spectroscopy and microscopy. Bio-binder solution dissolved in THF (10 mg/mL) was first centrifuged for 30 min in a Corning LSE Mini microcentrifuge (6000 rpm and 2000 RCF) to remove any particulates. Then, 800 μL of centrifuged Bio-binder solution was added to 12.6 mg of SiO_2 NPs and ultrasonicated for 30 min, after which it was left mostly undisturbed for one day. To rinse the treated SiO_2 NPs, the suspension was first centrifuged for 15 min and the supernatant discarded and replaced with 800 μL of clean THF. The solid pellet was ultrasonicated for at least 5 min until it was visibly disaggregated. Centrifugation and resuspension were repeated two more times, at which point the supernatant appeared mostly clear. After the last centrifugation, the pellet was dispersed in 800 μL of DI water, frozen in liquid nitrogen, and lyophilized on a Labconco FreeZone 6-Liter benchtop freeze dryer. A control sample of SiO_2 NPs was also subjected to the same process but only treated with clean THF.

UV-vis absorption spectra were collected on a Cary 6000i UV-vis-NIR spectrophotometer (Varian) and a quartz cuvette with 1 cm pathlength (28B-Q-10, Starna Cells). Absorption spectra of the SiO_2 NPs were obtained from suspensions of roughly 0.5 mg of nanoparticles in 600 μL of THF. The absorption spectra of Bio-binder and Bio-binder asphaltenes were measured from THF solutions that were diluted to 50 mg/L and centrifuged to remove particulates.

AFM and AFM-IR

To prepare the samples for atomic force microscopy (AFM), each filled capillary tube was first chilled for at least 20 min at -4 °C. Short segments of the tube were then snapped off under a stream of dry N_2 gas to prevent moisture condensation on the sample. Using a glass scribing tool to scribe the glass capillary before chilling also helped promote a clean, brittle fracture. The fractured segments were immediately mounted vertically and imaged under a large-stage 5600LS atomic force microscope (Keysight Technologies) in tapping mode with TAP-300 silicon cantilever tips (Budget Sensors, <10 nm nominal tip radius). Images were processed and analyzed with Gwyddion open-source software.

Chemical mapping by combined AFM and infrared (IR) absorption spectroscopy was performed using a demonstration model nanoIR3 system (Bruker Nano/Anasys Instruments) operating in tapping AFM-IR mode. The probes used for the experiments are standard tapping-mode AFM probes with overall gold coating (PR-EX-TnIR-C, Bruker Nano/Anasys Instruments) and nominal probe diameter ~20 nm. During the experiment, the sample chamber was continuously purged with clean dry air (CDA) to maintain ≤10% relative humidity. During spectral acquisition, multiple spectra were averaged at each site and smoothed using a Savitzky-Golay (3, 5) filter.

TEM imaging and EELS

High-resolution transmission electron microscopy images of Bio-binder-treated SiO_2 NPs (using ethanol instead of THF as the solvent) were captured using a JEOL 2010 FEG analytical electron microscope. For TEM imaging, SiO_2 NPs were briefly dispersed in ethanol and deposited on lacey carbon TEM grids by dip-coating and drying.

Electron energy loss spectroscopy (EELS) and the corresponding images were taken using a JEOL ARM microscope in STEM mode operated at 80kV. The low accelerating voltage was chosen to avoid electron beam damage to the SiO_2 particles. EELS were taken with a dispersion of 0.25 eV.

Kinetic adsorption experiments by *in situ* ATR-FTIR

In situ ATR-FTIR spectroscopy was used to evaluate the adsorption of Bio-binder onto silica nanoparticles (SiO_2 NPs). Kinetic measurements were collected on a Nicolet iS50 FTIR spectrometer (Thermo Fisher Scientific) with a ZnSe single reflection ATR crystal and flow cell adapter (PIKE Technologies, Fitchburg, WI). The instrument was set to average 200 spectral scans over a wavenumber range from (4000 to 800) cm^{-1} with a resolution of 2 cm^{-1}. SiO_2 NPs (5 g/L in acetone) was first dried onto the ATR crystal. After attaching the flow cell, THF was flowed over the NPs to remove loosely bound NPs, and a background spectrum in the solvent was acquired. Bio-binder (0.1% in THF) was then injected over the NPs using a glass syringe. Spectra were collected every 10 min for 3 h to monitor adsorption, while injecting from the syringe every 20 min to refresh the solution and maintain a 0.1% background (dissolved) Bio-binder concentration. Background subtraction was performed using the spectrum of the clean THF over NPs as the background.

An *ex situ* experiment was also conducted to independently confirm the adsorption identified in the *in situ* experiment. In this method, ≈ 10 mg of SiO_2 NPs was mixed with ≈ 17.8 mg of Bio-binder and 2 mL (1.78 g) of THF to achieve a 1% Bio-binder concentration. The sample was rotated end-over-end for 90 min, then the NPs were allowed to settle for 75 min. The supernatant THF was removed, and the Bio-binder-coated NPs were washed with ≈ 4 mL of clean THF. The settling and wash procedure was repeated four more times, after which the supernatant appeared clear. After removing the last wash solution, the NPs were deposited onto the ZnSe ATR crystal and allowed to dry. The clean, dry ZnSe crystal spectrum was subtracted as background to obtain the spectrum of the Bio-binder-coated NPs. A control was performed with only Bio-binder in THF (no NPs) to evaluate the possible contribution of poorly soluble Bio-binder species to the adsorbed Bio-binder spectra.

Reference spectra for the Bio-binder and three reference compounds (hexadecanamide, hexadecanamine, and palmitic acid) in THF were obtained using an ATR liquids retainer and volatiles cover (PIKE Technologies). After applying the reference compound as a powder, ~10 μL of THF was injected to induce better contact between the powder and the ATR crystal, and after solvent evaporation, the spectra of the dried compounds were collected. To collect the spectra of the dry Bio-binder, the sample was deposited onto the ATR crystal (without the addition of solvent) and spectra were collected. Dry compound spectra were processed with the clean, dry ATR crystal as the background. To obtain the spectra of the reference compounds or Bio-binder in THF, 0.15 mL of THF was injected on top of the dry sample, and the volatiles cover was installed to reduce evaporation. A pure liquid THF spectrum was subtracted as the background. The adsorption of the three reference compounds (1% in THF) onto SiO_2 NPs was also tested following the same method as the Bio-binder adsorption experiments. Only hexadecanamide showed spectral changes over time indicating adsorption.

Computational methods

To characterize the interaction and determine the affinity of Bio-binder molecules to silica, we calculated adsorption energies of selected Bio-binder molecules and ranked them based on their affinity for a model silica surface. For the computational analysis, periodic dispersion-corrected density functional theory (DFT-D) calculations were performed using the DMol3 module implemented in the Accelrys Materials Studio program package (version 6.0). The PBE (Perdew-Burke- Ernzerhof) formulation of generalized gradient approximation (GGA) was employed as the exchange-correlation density functional. Grimme's long-range dispersion correction is combined with the PBE functional (PBE-D) to treat van der Waals dispersion interactions.

"Fine" grid mesh points were specified for the matrix numerical integrations. All-electron double numerical basis sets augmented by polarization functions (DNP) and electron smearing of 0.005 hartree were also assigned. At this fine-level of DMol3 integration, the default k-point grid 1 × 2 × 1 was taken into consideration for Brillouin-zone integration. In geometry optimizations, the tolerances for energy, maximum force, and displacement convergence were 1.0×10^{-5} hartree, 2.0×10^{-3} hartree/Å, and 5.0×10^{-3} Å, respectively.

The adsorption energies, E_{ads}, for the adsorbate-silica surface interaction were calculated using the following equation, with the adsorbate being selected Bio-binder molecules:

$$E_{ads} = E_{Complex} - (E_{Silica} + E_{Adsorbate})$$

$E_{Complex}$ is the total energy of the optimized adsorption configuration, while E_{Silica} and $E_{Adsorbate}$ refer to the energy of a hydroxylated silica surface and the adsorbate, respectively. The more negative adsorption energy indicates stronger interaction of adsorbate with the silica surface. The optimized hydroxylated quartz (001) surface presented in Figure 1 was the model for the silica surface. As shown in this figure, two –OH groups have been connected to the top Si atom.

DFT-based molecular modeling of silica surface

The quartz (001) surface was cleaved on the basis of a primitive unit cell to generate reactive Si sites. The terminal atomic layer of the cleaved surface is a Si-rich termination. Fractured silica is highly hydrophilic, so that exposure to moisture results in surface hydrolysis with the formation of silanol groups until it becomes fully hydroxylated. Then, DFT calculations were carried out for the adsorption of selected compounds found in Bio-binder[23] on the fully hydroxylated (001) surface of α-quartz. This surface exhibits zigzag networks of hydrogen bonds with alternating weak and strong H-bonds due to the interaction between hydroxyl groups. This feature (shown as shaded-blue cavity in the top-view part of Figure 1) helps us detect the most probable sites to locate Bio-binder compounds and the other molecules in the complex.

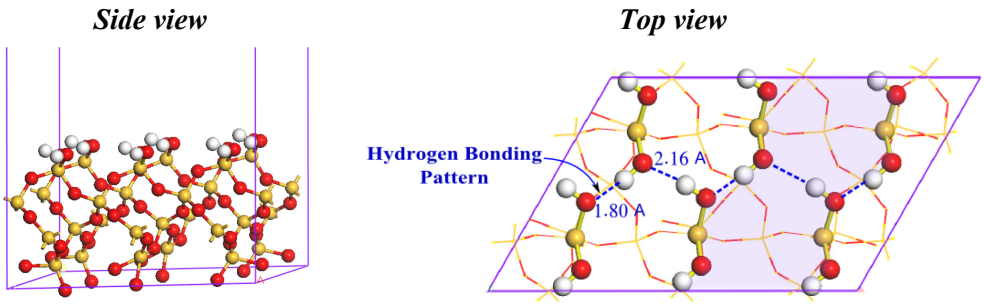

Figure 1. Model of hydroxylated quartz (001) surface. The hydrogen bonding network is presented in the top view.

RESULTS and DISCUSSION

Effect of external control mechanisms on migration of HDA to the interface

Figure 2 shows AFM images of the interface between acid-doped bitumen and glass surfaces. HDA crystals are seen growing off of clean glass surfaces (Fig. 2a), which is consistent with previous studies.[17] When the glass surface is modified with HMDS or APTES, HDA crystallization appeared to be completely suppressed (Fig. 2b and 2c). This result was especially surprising for HMDS, which only modifies the silica surface with a single-molecule layer of trimethylsilane groups. The fact that a molecular monolayer could entirely prevent micrometer-scale crystallization of HDA at the interface suggests that crystallization proceeds by a nucleation and growth mechanism in which crystal growth is dependent on and initiated by nucleation sites at the surface. The molecular structure of these surface nucleation sites is unknown but likely characterized by strong binding of HDA. Crystallization would deplete molecular HDA dissolved in the bitumen near the interface, driving diffusion of more HDA from the bulk toward the interface and enabling further crystal growth. Crystal growth and subsequent hydrolysis may not occur at all if the nucleation sites are neutralized. Therefore, any additive or surface modifier that can prevent HDA binding at the interface or compete for binding sites may improve bitumen's moisture resistance.

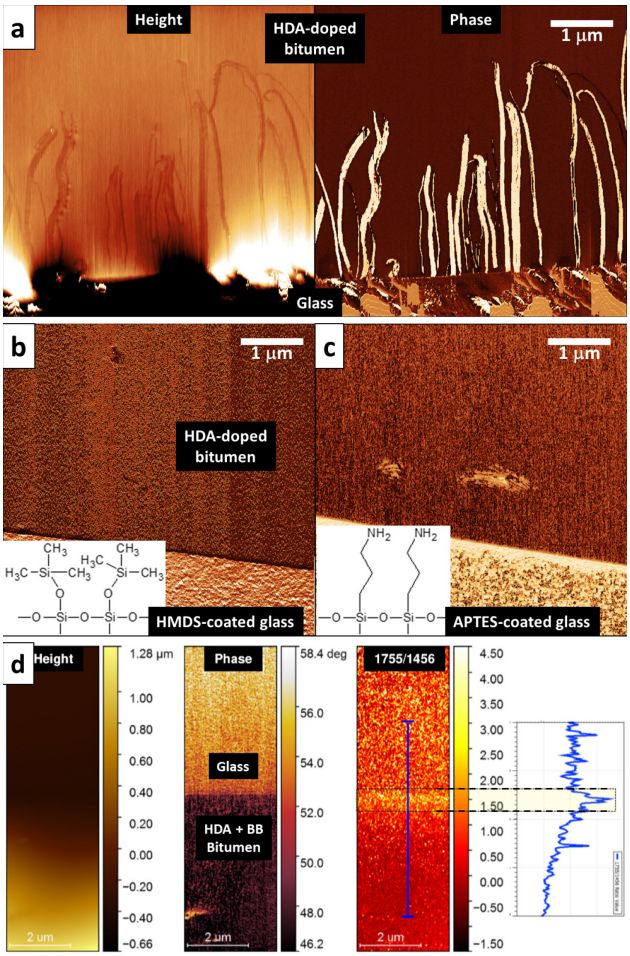

Figure 2. AFM images of the interface between 1 wt% HDA-doped bitumen and glass. (a) The interface with clean glass shows HDA crystals. Phase images of the interface with (b) HMDS-coated glass and (c) APTES-coated glass show no crystals. (d) AFM-IR images of the interface between clean glass and HDA-doped bitumen containing Bio-binder also show the absence of HDA crystals. An image of the ratio of IR absorbance at 1755 cm^{-1} versus 1456 cm^{-1} suggests an enrichment of carbonyl groups around the interface.

It should be noted that use of HMDS and APTES as model compunds in this paper was to allow accurate invetsigation of surface passivation mechanisms; neither of them are recommended as adhesion promotors for asphalt concrete in practice. In fact, HMDS does prevent binding of acidic compounds to the interface, but it could also prevent binding of other macromolecules in bitumen that might otherwise promote adhesion. APTES presents amine groups that bitumen macromolecules could bind to, but those amine groups are also known to catalyze self-hydrolysis of APTES off of the the silica surface over time.[25] Therefore, to ensure desirable adhesion, it is critical to use liquid dopants that not only have high affinity for siliceous surfaces but also are resistant to hydrolysis and compatible with asphalt molecules.

AFM-IR of HDA-doped bitumen containing Bio-binder

As a less expensive alternative to commercial chemical anti-stripping agents, Bio-binder made from waste bio-mass was examined for its impact on bitumen's interfacial microstructure.[22,23] Bio-binder is compatible with asphalt[23] and improves asphalt's resistance to moisture.[26] Figure 2d shows AFM-IR images of the glass interface with HDA-doped bitumen containing Bio-binder. Height and phase images show that the addition of 1 wt% Bio-binder completely suppresses HDA crystal growth at the interface. IR absorption images taken at 1755 cm^{-1} and 1456 cm^{-1} suggest the possible enrichment of carbonyl groups in a layer approximately 200 nm thick at the interface. Carbonyl absorption at 1755 cm^{-1} tends to be related to ketone groups, but closer examination of the IR absorption spectra shows somewhat broad absorbance in that region that may be indicative of the presence of a variety of different carbonyl groups (Supplemental Information, Figure S1). However, the supposed enrichment is not definitive and requires further examination in a future study.

Based on the results obtained for silanized glass, it is plausible that Bio-binder suppresses HDA crystallization in a similar manner by binding to the surface and neutralizing any nucleation sites before HDA can bind to the glass. Bio-binder is a complex mixture of many chemical compounds,[22-23] and identifying the specific components that are surface active would be invaluable information for optimizing the Bio-binder formulation. The experiment also demonstrates the utility of HDA-doped bitumen as a model compound for studying the efficacy of new anti-stripping agents. As a minimum requirement, effective anti-stripping agents for siliceous stones should be able to displace carboxylic acids from the interface and consequently completely suppress the appearance of any crystallized HDA microstructure there.

Adsorption of Bio-binder compounds to the silica interface

In an effort to identify the Bio-binder compounds that bind most tightly to silica surfaces, SiO_2 NPs were treated with Bio-binder solution and characterized by TEM imaging, EELS, and absorption spectroscopy; the results are shown in Figure 3. Bio-binder-treated SiO_2 NPs retain a brown color even after washing with THF. This color is likely due to polyaromatic hydrocarbons from the Bio-binder adsorbing to silica. The UV-visible absorption spectra of whole Bio-binder and isolated Bio-binder “asphaltenes” dispersed in THF are shown in Fig. 3a. The stronger absorption by the “asphaltenes” at longer wavelengths is indicative of larger or more aggregated polyaromatic structures.[27-30] Similarly, the absorption spectrum of Bio-binder-treated SiO_2 NPs also shows strong absorption in the visible range (400-700 nm) relative to the absorption in the UV range (300-400 nm). UV-vis spectroscopy cannot accurately identify the compounds that are adsorbed, because of shifts in the absorption spectra due to aggregation and binding to silica, as well as Rayleigh scattering by the SiO_2 NPs. However, the data show that the Bio-binder adsorbates include a significant quantity of polyaromatic compounds. In comparison, SiO_2 NPs treated with bitumen dissolved in THF show a much weaker overall absorbance than the Bio-binder-treated NPs. This result suggests that the compounds that adsorb to the silica from native bitumen either possess smaller PAH cores or adsorb in thinner or incomplete layers compared to Bio-binder adsorbates. A thicker adsorbate layer observed in Bio-binder treated SiO_2 NPs could indicate stronger binding to the silica surface and may also offer a more favorable interface for connecting with non-adsorbing bitumen constituents, thereby improving adhesion strength.

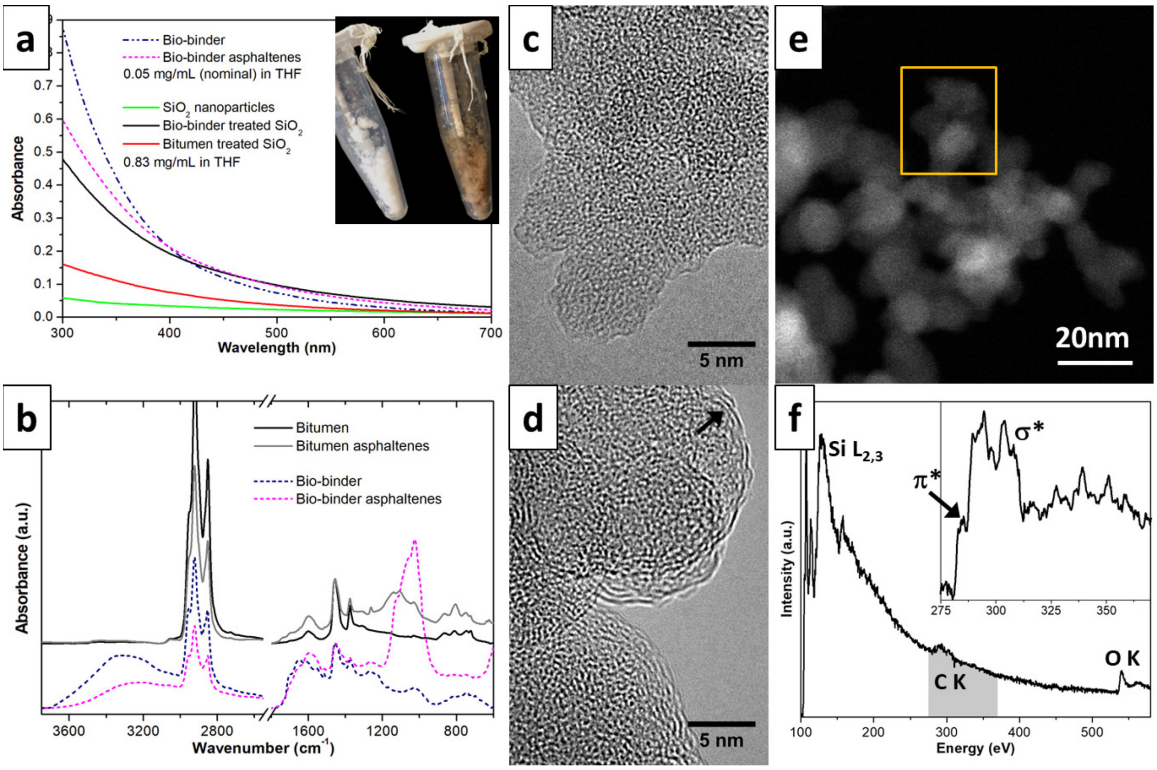

Figure 3. (a) UV-vis spectra and photograph of SiO_2 NPs and Bio-binder-treated SiO_2 NPs. Brown color and absorption spectra are consistent with the presence of polyaromatic hydrocarbons such as those found in asphaltenes. (b) ATR-FTIR of bitumen, Bio-binder, and extracted "asphaltenes" from both. Bio-binder shows a greater proportion of polar groups compared to bitumen. Spectra were normalized to the peak at 1456 cm^{-1} and offset for clarity. (c, d) HRTEM images of clean SiO_2 NPs (c) and Bio-binder treated SiO_2 NPs (d) also suggest the presence of molecular layers (black arrow) consistent with flat and stacked polyaromatic compounds. (e) STEM image of Bio-binder-treated SiO_2 NPs and (f) EELS spectrum of a selected area (yellow box) confirm the presence of sp2 carbon around the nanoparticles.

UV-vis spectroscopy does not provide any data on the relative abundance of saturated versus unsaturated hydrocarbons adsorbed to silica, because saturated hydrocarbons do not absorb much light. HRTEM images of similar Bio-binder-treated nanoparticles suggest the presence of a layered molecular coating on the SiO_2 NPs that is consistent with planar polyaromatic compounds lying flat against the silica surface with a layer spacing of approximately 0.3 – 0.4 nm. EELS measurements (Fig. 3f) of carbon K edge energy loss near edge structure (ELNES) show the presence of a π* peak, confirming the sp2 bonded nature of the surface hydrocarbon. The quantitative estimate of carbon concentration based on the EELS measurement gives an atomic ratio of C/Si of about 9%. Both Bio-binder and Bio-binder "asphaltenes" contain more polar groups than bitumen or bitumen asphaltenes, as evidenced by FTIR absorption signatures around 3500 – 3000 cm^{-1} (OH/NH stretch), 1800 – 1650 cm^{-1} (C=O stretch), and 1300 – 900 cm^{-1} (various oxygen groups and other bands); this is consistent with previous measurements.[31] From the relative heights of the aliphatic peaks around 3000 – 2800 cm^{-1}, Bio-binder "asphaltenes" are also comparatively deficient in alkane groups. The large peak at 1026 cm^{-1} may be due to silica impurities in the Bio-binder "asphaltene" sample.

Nascimento et al.[32] showed that within a petroleum asphaltene fraction, the species that bound to silica strongest tended to be the smaller polyaromatics that contained polar groups.

Bitumen asphaltenes that lack similar polar groups may adsorb, but it has been suggested that they also may be more easily displaced by water.[33-34] UV-vis absorption measurements of the Bio-binder-treated SiO_2 NPs and bitumen-treated SiO_2 NPs after washing with water did not detect significant removal of polyaromatic adsorbates from either sample (Supplemental Information Figure S2). It is hypothesized that strong binding of Bio-binder polyaromatic compounds results from multiple polar groups that can directly bond with the silica surface, in addition to strong dispersion interactions across a large area of contact when these Bio-binder polyaromatic compounds lie flat against the surface. Petroleum asphaltenes are known to organize parallel to oil-water interfaces as well,[35] although it remains to be definitively proven that parallel rather than perpendicular stacking of asphaltenes predominates at realistic bitumen-aggregate interfaces.

Modeling of molecular adsorption over the silica surface

Figure 4 shows models of selected molecules with different functional groups previously identified in Bio-binder.[23] These models are referred to as BioBs. To investigate the nature and strength of interactions between BioBs and the hydroxylated silica surface, truncated BioB candidates (T-BioBs) were inserted into the space on top of the surface. Hydroxyl sites on the silica surface are most likely to interact with polar functional groups of the adsorbates. The results of calculated interaction energies are reported in Figure 5 and in Supplemental Information, Table S1. In all complexes, an adsorbate molecule interacts with the surface through the formation of hydrogen bonding between its polar head and the silica hydroxyl groups. The adsorption energies given in Figure 5 show that the strongest adsorption on the silica surface is by T-BioB10, truncated α-tocopherol (the most biologically active form of vitamin E), via hydrogen bonding with the phenol group, E_{ads}=-51.9 kcal/mol. The second strongest binding was exhibited by APTES (-36.3 kcal/mol), which was modeled as a surrogate for amine-containing compounds for comparison. While primary amine groups are not so prevalent in Bio-binder, amide compounds are common and include the primary alkyl amide BioB1, which shows a stronger binding to silica (T-BioB1, -28.4 kcal/mol) than the alkyl carboxylic acid fragment (T-BioB6, -21.3 kcal/mol).

Models of the adsorbate molecules were truncated to reduce the length of akyl chains, in order to decrease the computational cost. In order to examine the effect of alkyl chain size on adsorption, a DFT simulation was carried out separately for T-BioB6 with a longer alkyl chain (T-L-BioB6). Increasing the number of carbon atoms from C_8 to C_{10} increased the interaction energy from -21.3 to -23.5 kcal/mol. This effect could be due to the electron-donating nature of an alkyl group attached to the functional group, which increases the charge difference in the polar head of a molecule through an inductive effect, leading to stronger adsorption with a longer alkyl chain, up to a certain point. Importantly, a further increase in the number of carbon atoms did not show a significant further increase in the adsorption energy. Therefore, the truncated BioBs were deemed appropriate for computational modeling of BioBs.

While it is important to remember that these binding energies were calculated for adsorbates under vacuum, the fact that the strongest binding was observed for BioB10 and APTES is intriguing in light of other published work. Research on marine mussels shows that the protein glue they use to adhere themselves to rocks even under seawater is rich in the catecholic amino acid, 3,4-dihydroxyphenylalanine, as well as the amine-terminated amino acid, lysine (Supplemental Information, Figure S3).[18-19, 36] The anionic and non-polar residues found in mussel foot proteins are also believed to play important roles in adhesion and cohesion, and such

insights could be useful for rational design of Bio-binder-based adhesion promoters for asphalt concrete. In addition, vitamin E has also been studied as an anti-aging additive in bitumen.[37]

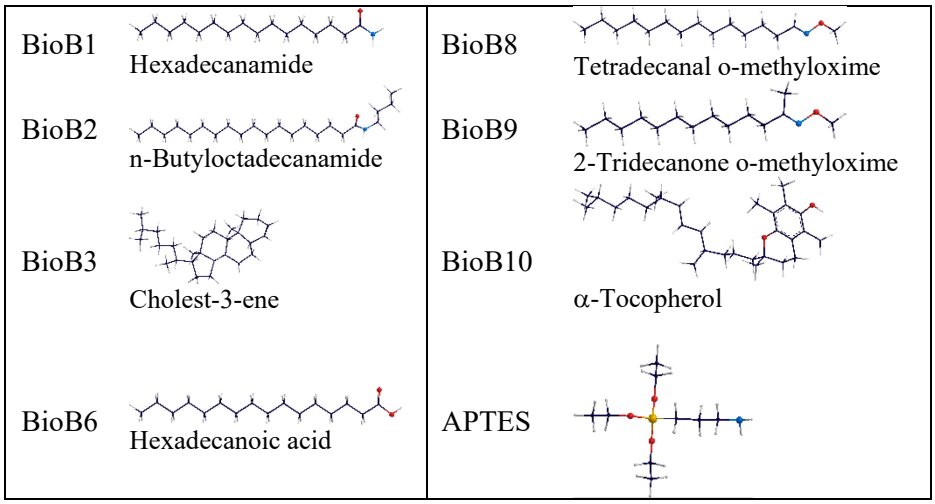

Figure 4. Models of adsorbate molecules.

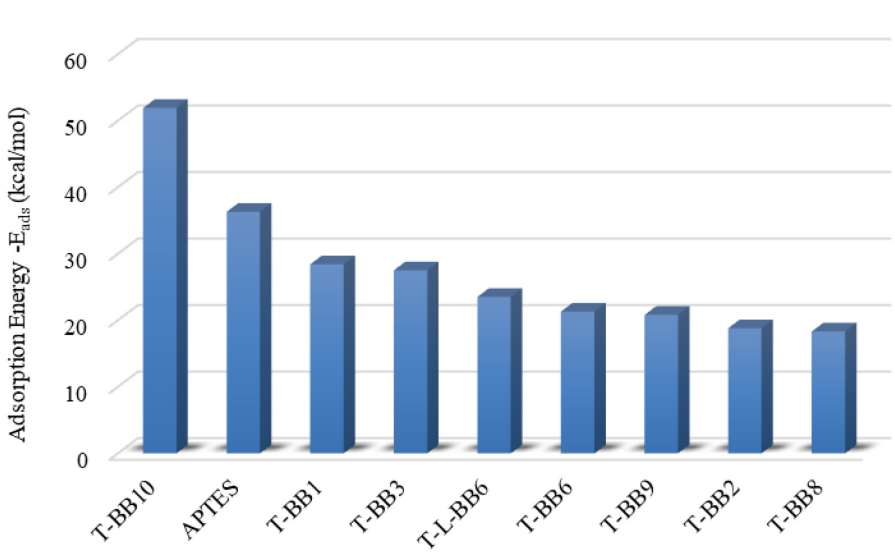

Figure 5. Adsorption energies ($-E_{ads}$) of molecular adsorbates over a hydroxylated quartz (001) surface.

Kinetic adsorption experiments by in situ ATR-FTIR

In situ ATR-FTIR measurements were carried out in order to better characterize the chemical constituents of Bio-binder that adsorb to silica (Figure 6). For the quantitative analysis, the absorbance at 2000 cm^{-1} was used as the baseline for the spectral region 2000 – 1300 cm^{-1}, and the absorbance at 4000 cm^{-1} was used as the baseline for the spectral region 4000 – 3000 cm^{-1}. The alkyl C–H stretch region (3100 – 2800 cm^{-1}) and the region from 1200 – 800 cm^{-1} were not included in the analysis due to contributions from the THF solvent and the SiO_2 NPs.

Preferential adsorption of certain fractions of Bio-binder onto the SiO_2 NPs over time was indicated by increasing absorbance of only some, but not all, peaks observed in the ATR-

FTIR spectrum of the complete Bio-binder mixture (Figure 6). The DFT results show that the α-tocopherol (BioB10) and hexadecanamide (BioB1) compounds present in Bio-binder have high affinities toward silica, and polyaromatic Bio-binder adsorbates are also likely to possess amide and phenol groups. Therefore, we specifically evaluated whether the *in situ* ATR-FTIR data on the competitive adsorption of specific functional groups from the entire Bio-binder mixture would be consistent with these results, or whether other species present in the complex mixture would interfere with the binding of T-BioB10 and T-BioB1.

The main peaks observed to adsorb from the Bio-binder (Figure 6) are consistent with prior FTIR studies on Bio-binder.[22, 36] The adsorbing peaks around 1590 cm^{-1} and 1440 cm^{-1} have most commonly been attributed to aromatic C=C stretching[39-44] and symmetric aliphatic CH_2 or CH_3 bending modes,[32, 43-45] respectively, and the observation of their adsorption is also consistent with a prior study on the adsorption of asphaltene onto silica.[32] The broad peak at 3500 – 3100 cm^{-1} is attributed primarily to hydroxyl groups[40, 46-47] and is also in agreement with the irreversible adsorption of OH groups of asphaltene onto silica in a previous study.[32] The shoulder around 1690 cm^{-1} is in the region attributed to C=O stretches. The results for the Bio-binder-coated SiO_2 NPs that were prepared and washed *ex situ* confirm that the adsorbed species in the flow cell experiment are strongly bound to the SiO_2 (Figure S4(a)) and are not related to deposition of poorly-soluble Bio-binder, which shows a different spectrum than the adsorbed species (Figure S4(b)).

Since the C=O peak can arise from a number of different functional groups, in order to more confidently evaluate whether the 1690 cm^{-1} shoulder is related to the hypothesized T-BioB1 amide adsorption, additional adsorption experiments were performed with three pure reference compounds: hexadecanamine, hexadecanamide (BioB1), and HDA (BioB6). No significant adsorption was observed for either hexadecanamine or HDA (data not shown). The fact that hexadecanamine showed no adsorption whereas the amine group showed the second strongest binding to silica by DFT may be due to the difference between the DFT models of compounds in a vacuum versus adsorption experiments performed in THF. In comparison, hexadecanamide peaks at 1464 cm^{-1} (C–N stretching),1609 cm^{-1} (N–H bending), and 1690 cm^{-1}(C=O stretching) as well as peaks at 3216 and 3338 cm^{-1}(N–H stretching) were observed to adsorb onto SiO_2 (Figure S7). The time-resolved results also suggest that fast initial adsorption of the amide onto SiO_2 is followed by increasing interaction over time of specifically the N–H bonds, which show changing peak height ratios over time as well as peak shifts relative to the hexadecanamide dissolved in THF (Figure S6). Having confirmed both the C=O peak location as well as the amide interaction with SiO_2 for hexadecanamide, the 1690 cm^{-1} absorbance in the Bio-binder adsorption (Figure 6) can then be considered consistent with amide species adsorbing from the Bio-binder, where the expected amide N–H stretches at 3338 cm^{-1} and 3216 cm^{-1} and the expected N–H bending at 1609 cm^{-1} observed in the adsorbing hexadecanamide reference compound may be obscured by the O–H and C=C peaks. However, note that by comparing the adsorbing species to the spectrum of the complete Bio-binder dissolved in THF, the adsorption of carboxyl species in general from 1750 to 1630 cm^{-1} from the complete Bio-binder mixture appears to be relatively less favorable than adsorption of the OH and C=C components.

Finally, the time-resolved adsorption profiles of the various functional groups in Figure 6 were compared (Figure 7). Interestingly, the adsorption kinetics of the OH groups differ from those of the C=O, C=C, and aliphatic CH groups. The C=O, C=C, and CH absorbances follow each other and begin to plateau together over 3 h, while the OH groups continue to adsorb

increasingly relative to the C=C groups. These results are consistent with the DFT prediction of stronger affinities of T-BioB10 (containing an OH functionality) relative to the other major species in the Bio-binder. Also, the results are consistent with multilayer or self-stacking of alcohol groups over time. Another possibility is that these trends illustrate a kinetic reorganization of adsorbates with time. Small-molecule adsorbates diffuse quickly and can bind immediately, but they can eventually be displaced by larger molecules that diffuse slowly but bind more strongly. A similar time-dependent effect is thought to affect the adsorption of petroleum asphaltenes to oil-water interfaces and the subsequent stabilization of oil-water emulsions.[35]

The TEM, UV-vis absorption, and FTIR data confirm the adsorption of polar polyaromatics to silica that, due to their low volatility and high molecular weight, are not represented by the list of BioB compounds identified by gas chromatography.[23] However, those polyaromatics likely possess many of the same chemical functional groups exhibited by the compounds on that list, and the mixture of different chemical groups may work together to strengthen adhesion on a variety of mineral surfaces. The small-molecule BioB compounds may also diffuse to the interface first, taking part in the initial adsorption process or acting as plasticizers to facilitate conformational coating and flow of bitumen into aggregate pores at the surface.

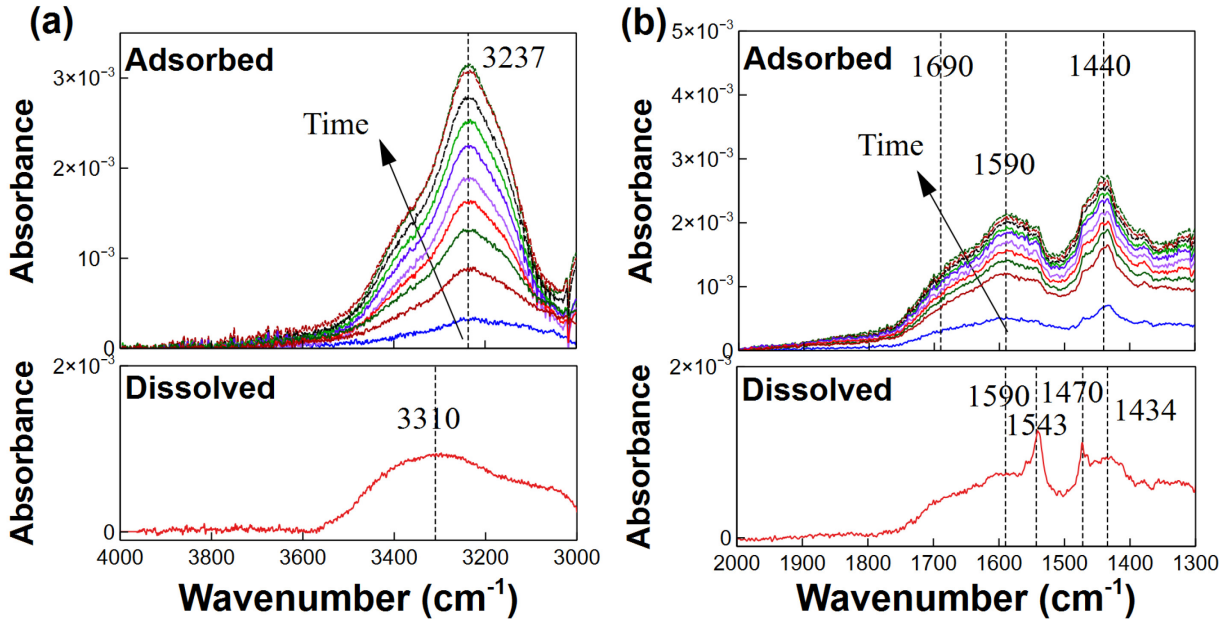

Figure 6. *In situ* ATR-FTIR experiment for adsorption of Bio-binder (0.1% in THF) over SiO_2 NPs. The spectra are displayed in 20 minute intervals from 0 to 180 minutes and were processed by background subtraction of pure THF over the NPs. The bottom figures show the reference spectra of the complete biobinder in THF (no NPs) after background subtraction of pure THF. All spectra were vertically aligned at 4000 cm^{-1} in (a) and 2000 cm^{-1} in (b) but otherwise are presented at a common scale. Consistent trends were also observed in adsorption experiments with 1% Bio-binder.

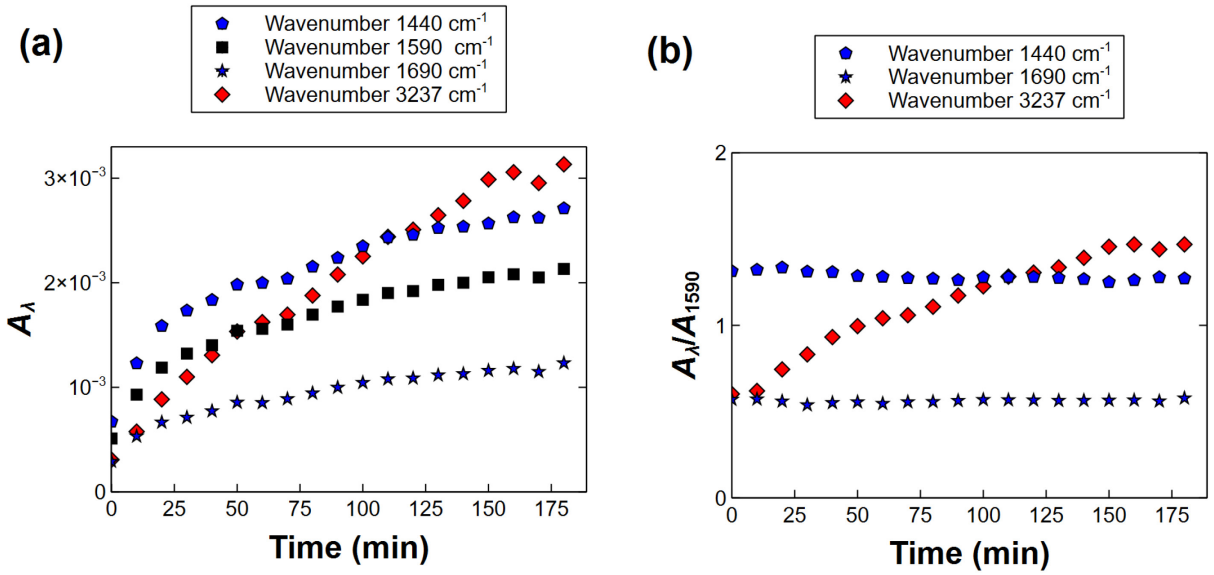

Figure 7. (a) Peak heights at wavenumbers of 3237, 1690, 1590, and 1440 cm^{-1} during the adsorption of Bio-binder onto SiO_2 NPs, and (b) ratios of peak heights to identify similarities or differences in adsorption kinetics relative to 1590 cm^{-1}.

CONCLUSIONS

Adhesive failure at the bitumen-aggregate interface is one of the most prevalent forms of pavement distress. This study used AFM, TEM, absorption spectroscopy, and computational modeling to examine the chemistry and molecular mechanisms by which selected surface passivating agents bind to a mineral surface. This knowledge is important for developing strategies to improve pavements' durability and resistance to damage from moisture.

Carboxylic acid compounds have been linked to increased susceptibility to moisture damage; their accumulation and crystallization at the interface of bitumen and siliceous stone aggregates can give rise to subsequent hydrolysis promoting moisture damage in pavements. HDA-doped bitumen was found to be a useful model compound for examining the binding of acids to silica at an interface. The binding of HDA to active sites on the silica surface nucleates crystals of HDA to grow at the interface, as seen by AFM imaging. The Bio-binder used as a liquid dopant completely suppressed HDA crystallization, presumably by binding to these active sites tightly and blocking HDA adsorption. This in turn, can prevent subsequent hydrolysis at the interface of bitumen and stone aggregates mitigating its susceptibility to moisture damage. This observation is consistent with previous results showing that Bio-binder can improve pavements' resistance to moisture damage.[26] TEM and UV-vis spectroscopy suggest that polar polyaromatic Bio-binder molecules akin to "asphaltenes" are the primary adsorbate species. DFT analysis and *in-situ* FTIR showed selective adsorption of Bio-binder molecules onto the silica surface, with hydroxyl groups showing the highest binding energy followed by amide functional groups. Adhesion depends on a chain of multiple molecular bonds that link the mineral surface to whole bitumen, and more in-depth characterization of each link enables identification of weak points and possible methods for strengthening the chain. Future studies will focus on more rigorous chemical identification and mapping of Bio-binder adsorbates at stone aggregates surfaces. The results of this study highlight the importance of integrating chemical mapping in the pavement

design and engineering phase to mitigate occurrence of moisture damage during pavement service life.

ACKNOWLEDGMENTS

This research is sponsored by the National Science Foundation (Award Numbers 1150695 and 1546921). The authors thank Dr. Anirban Roy, Thomas (Taiye) Zhang, and Dr. Qichi Hu from Bruker Nano Surfaces for their help with the AFM-IR demonstration. The authors thank Dr. Shiahn Chen from the MIT Materials Research Laboratory for assistance with TEM imaging. The authors thank Dr. Jenni Briggs from Pike Technologies for the use of ATR-FTIR accessories. The authors are grateful for the access to instrumentation at the Joint School of Nanoscience and Nanoengineering and for the support from the State of North Carolina. The contents of this paper reflect the view of the authors, who are responsible for the facts and the accuracy of the data presented.

REFERENCES

1. Antunes, V.; Freire, A. C.; Quaresma, L.; Micaelo, R., Influence of the geometrical and physical properties of filler in the filler–bitumen interaction. *Construction and Building Materials* **2015,** *76*, 322-329.
2. Antunes, V.; Freire, A. C.; Quaresma, L.; Micaelo, R., Effect of the chemical composition of fillers in the filler–bitumen interaction. *Construction and Building Materials* **2016,** *104*, 85-91.
3. Guo, M.; Tan, Y.; Yu, J.; Hou, Y.; Wang, L., A direct characterization of interfacial interaction between asphalt binder and mineral fillers by atomic force microscopy. *Mater Struct* **2017,** *50* (2), 141.
4. Hesami, E.; Birgisson, B.; Kringos, N., Numerical and experimental evaluation of the influence of the filler–bitumen interface in mastics. *Mater Struct* **2014,** *47* (8), 1325-1337.
5. Adams, J. J., Asphaltene Adsorption, a Literature Review. *Energy & Fuels* **2014,** *28* (5), 2831-2856.
6. Akbarzadeh, K.; Hammami, A.; Kharrat, A.; Zhang, D.; Allenson, S.; Creek, J.; Kabir, S.; Jamaluddin, A.; Marshall, A. G.; Rodgers, R. P., Asphaltenes—problematic but rich in potential. *Oilfield Review* **2007,** *19* (2), 22-43.
7. Chacón-Patiño, M. L.; Rowland, S. M.; Rodgers, R. P., Advances in Asphaltene Petroleomics. Part 1: Asphaltenes Are Composed of Abundant Island and Archipelago Structural Motifs. *Energy & Fuels* **2017,** *31* (12), 13509-13518.
8. Chacón-Patiño, M. L.; Rowland, S. M.; Rodgers, R. P., Advances in Asphaltene Petroleomics. Part 2: Selective Separation Method That Reveals Fractions Enriched in Island and Archipelago Structural Motifs by Mass Spectrometry. *Energy & Fuels* **2018,** *32* (1), 314-328.
9. Chacón-Patiño, M. L.; Rowland, S. M.; Rodgers, R. P., Advances in Asphaltene Petroleomics. Part 3. Dominance of Island or Archipelago Structural Motif Is Sample Dependent. *Energy & Fuels* **2018,** *32* (9), 9106-9120.
10. Lesueur, D.; Petit, J.; Ritter, H.-J., The mechanisms of hydrated lime modification of asphalt mixtures: a state-of-the-art review. *Road Materials and Pavement Design* **2013,** *14* (1), 1-16.
11. Plancher, H.; Green, E. L.; Petersen, J. C., Reduction of oxidative hardening of asphalts by treatment with hydrated lime – a mechanistic study. *Proceedings of the Association of Asphalt Paving Technologists* **1976,** *45*, 1-24.
12. Airey, G. D.; Collop, A. C.; Zoorob, S. E.; Elliott, R. C., The influence of aggregate, filler and bitumen on asphalt mixture moisture damage. *Construction and Building Materials* **2008,** *22* (9), 2015-2024.

13. Buddhala, A.; Hossain, Z.; Wasiuddin, N.; Zaman, M.; rsquo; Rear, E., Effects of an Amine Anti-Stripping Agent on Moisture Susceptibility of Sasobit and Aspha-Min Mixes by Surface Free Energy Analysis. *Journal of Testing and Evaluation* **2012,** *40*, JTE103618.
14. Cui, S.; Blackman, B. R. K.; Kinloch, A. J.; Taylor, A. C., Durability of asphalt mixtures: Effect of aggregate type and adhesion promoters. *International Journal of Adhesion and Adhesives* **2014,** *54*, 100-111.
15. Arabani, M.; Hamedi, G. H., Using the surface free energy method to evaluate the effects of liquid antistrip additives on moisture sensitivity in hot mix asphalt. *International Journal of Pavement Engineering* **2014,** *15* (1), 66-78.
16. Xiao, F.; Amirkhanian, S. N., Effects of liquid antistrip additives on rheology and moisture susceptibility of water bearing warm mixtures. *Construction and Building Materials* **2010,** *24* (9), 1649-1655.
17. Hung, A. M.; Mousavi, M.; Pahlavan, F.; Fini, E. H., Intermolecular Interactions of Isolated Bio-Oil Compounds and Their Effect on Bitumen Interfaces. *ACS Sustainable Chemistry & Engineering* **2017,** *5* (9), 7920-7931.
18. Ahn, B. K.; Das, S.; Linstadt, R.; Kaufman, Y.; Martinez-Rodriguez, N. R.; Mirshafian, R.; Kesselman, E.; Talmon, Y.; Lipshutz, B. H.; Israelachvili, J. N.; Waite, J. H., High-performance mussel-inspired adhesives of reduced complexity. *Nature Communications* **2015,** *6*, 8663.
19. Ding, Y. H.; Floren, M.; Tan, W., Mussel-inspired polydopamine for bio-surface functionalization. *Biosurface and Biotribology* **2016,** *2* (4), 121-136.
20. Lee, H.; Dellatore, S. M.; Miller, W. M.; Messersmith, P. B., Mussel-Inspired Surface Chemistry for Multifunctional Coatings. *Science* **2007,** *318* (5849), 426-430.
21. Samieadel, A.; Schimmel, K.; **Fini**, E.H., Comparative Life Cycle Assessment (LCA) of Bio-Modified Binder and Conventional Asphalt Binder, *Clean Technologies and Environmental Policy* **2018**, 20(1): 191–200.
22. Hosseinnezhad, S.; Fini, E. H.; Sharma, B. K.; Basti, M.; Kunwar, B., Physiochemical characterization of synthetic bio-oils produced from bio-mass: a sustainable source for construction bio-adhesives. *RSC Advances* **2015,** *5* (92), 75519-75527.
23. Fini, E. H.; Kalberer, E. W.; Shahbazi, A.; Basti, M.; You, Z.; Ozer, H.; Aurangzeb, Q., Chemical Characterization of Biobinder from Swine Manure: Sustainable Modifier for Asphalt Binder. *Journal of Materials in Civil Engineering* **2011,** *23* (11), 1506-1513.
24. Fini, E. H.; Hosseinnezhad, S.; Oldham, D. J.; Chailleux, E.; Gaudefroy, V., Source dependency of rheological and surface characteristics of bio-modified asphalts. *Road Materials and Pavement Design* **2016**, 1-17.
25. Zhu, M.; Lerum, M. Z.; Chen, W., How To Prepare Reproducible, Homogeneous, and Hydrolytically Stable Aminosilane-Derived Layers on Silica. *Langmuir* **2012,** *28* (1), 416-423.
26. Oldham, D.; Yaya, A.; Folley, D.; Fini, E., Effects of warm mix additives on asphalt moisture resistance. In *Transporation Research Board Conference*, Washington DC, **2017**; Vol. 17-05541, pp 17-05541.
27. Evdokimov, I. N.; Eliseev, N. Y.; Akhmetov, B. R., Assembly of asphaltene molecular aggregates as studied by near-UV/visible spectroscopy: I. Structure of the absorbance spectrum. *Journal of Petroleum Science and Engineering* **2003,** *37* (3), 135-143.
28. Friedel, R. A.; Orchin, M., *Ultraviolet spectra of aromatic compounds*. Wiley New York: **1951**; Vol. 40.
29. Groenzin, H.; Mullins, O. C., Molecular Size and Structure of Asphaltenes from Various Sources. *Energy & Fuels* **2000,** *14* (3), 677-684.
30. Ruiz-Morales, Y.; Mullins, O. C., Measured and Simulated Electronic Absorption and Emission Spectra of Asphaltenes. *Energy & Fuels* **2009,** *23* (3), 1169-1177.

31. Pahlavan, F.; Hung, A.; Fini, E. H., Evolution of molecular packing and rheology in asphalt binder during rejuvenation. *Fuel* **2018,** *222*, 457-464.
32. Nascimento, P. T. H.; Santos, A. F.; Yamamoto, C. I.; Tose, L. V.; Barros, E. V.; Gonçalves, G. R.; Freitas, J. C. C.; Vaz, B. G.; Romão, W.; Scheer, A. P., Fractionation of Asphaltene by Adsorption onto Silica and Chemical Characterization by Atmospheric Pressure Photoionization Fourier Transform Ion Cyclotron Resonance Mass Spectrometry, Fourier Transform Infrared Spectroscopy Coupled to Attenuated Total Reflectance, and Proton Nuclear Magnetic Resonance. *Energy & Fuels* **2016,** *30* (7), 5439-5448.
33. Curtis, C. W.; Ensley, K.; Epps, J. *Fundamental properties of asphalt-aggregate interactions including adhesion and absorption*; SHRP-A-341; National Research Council Washington, DC: **1993**.
34. Fritschy, G.; Papirer, E., Interactions between a bitumen, its components and model fillers. *Fuel* **1978,** *57* (11), 701-704.
35. Liu, F.; Darjani, S.; Akhmetkhanova, N.; Maldarelli, C.; Banerjee, S.; Pauchard, V., Mixture Effect on the Dilatation Rheology of Asphaltenes-Laden Interfaces. *Langmuir* **2017,** *33* (8), 1927-1942.
36. Lee, B. P.; Messersmith, P. B.; Israelachvili, J. N.; Waite, J. H., Mussel-Inspired Adhesives and Coatings. *Annual Review of Materials Research* **2011,** *41* (1), 99-132.
37. Apeagyei, A. K., Laboratory evaluation of antioxidants for asphalt binders. *Construction and Building Materials* **2011,** *25* (1), 47-53.
38. Fini, E. H.; Høgsaa, B.; Christiansen, J. d. C.; Sanporean, C.-G.; Jensen, E. A.; Mousavi, M.; Pahlavan, F., Multiscale Investigation of a Bioresidue as a Novel Intercalant for Sodium Montmorillonite. *The Journal of Physical Chemistry C* **2017,** *121* (3), 1794-1802.
39. Calemma, V.; Iwanski, P.; Nali, M.; Scotti, R.; Montanari, L., Structural Characterization of Asphaltenes of Different Origins. *Energy & Fuels* **1995,** *9* (2), 225-230.
40. Moschopedis, S. E.; Speight, J. G., Oxygen functions in asphaltenes. *Fuel* **1976,** *55* (4), 334-336.
41. Russo, C.; Stanzione, F.; Tregrossi, A.; Ciajolo, A., Infrared spectroscopy of some carbon-based materials relevant in combustion: Qualitative and quantitative analysis of hydrogen. *Carbon* **2014,** *74*, 127-138.
42. Chang, C.-L.; Fogler, H. S., Stabilization of Asphaltenes in Aliphatic Solvents Using Alkylbenzene-Derived Amphiphiles. 1. Effect of the Chemical Structure of Amphiphiles on Asphaltene Stabilization. *Langmuir* **1994,** *10* (6), 1749-1757.
43. Wilt, B. K.; Welch, W. T.; Rankin, J. G., Determination of Asphaltenes in Petroleum Crude Oils by Fourier Transform Infrared Spectroscopy. *Energy & Fuels* **1998,** *12* (5), 1008-1012.
44. Suryanarayana, I.; Rao, K. V.; Duttachaudhury, S. R.; Subrahmanyam, B.; Saikia, B. K., Infrared spectroscopic studies on the interactions of pour point depressants with asphaltene, resin and wax fractions of Bombay high crude. *Fuel* **1990,** *69* (12), 1546-1551.
45. Charlesworth, J. M., Influence of temperature on the hydrogenation of Australian Loy-Yang brown coal. 2. Structural analysis of the asphaltene fractions. *Fuel* **1980,** *59* (12), 865-870.
46. Chen, C.; Gao, J.-S.; Yan, Y.-J., Original preasphaltenes and asphaltenes in coals. *Fuel Processing Technology* **1998,** *55* (2), 143-151.
47. Ignasiak, T.; Strausz, O. P.; Montgomery, D. S., Oxygen distribution and hydrogen bonding in Athabasca asphaltene. *Fuel* **1977,** *56* (4), 359-365.